MOLECULAR AND CELLULAR BIOLOGY, July 2007, p. 5029–5039 Vol. 27, No. 13
0270-7306/07/$08.00+0 doi:10.1128/MCB.01566-06

Essential Role of Ubiquitin-Specific Protease 8 for Receptor Tyrosine Kinase Stability and Endocytic Trafficking In Vivo▽†

Sandra Niendorf,[1] Alexander Oksche,[2] Agnes Kisser,[1] Jürgen Löhler,[3] Marco Prinz,[4] Hubert Schorle,[5] Stephan Feller,[6] Marc Lewitzky,[6] Ivan Horak,[1] and Klaus-Peter Knobeloch[1]*

Leibniz Institut für Molekulare Pharmakologie, Abteilung Molekulare Genetik, Krahmerstr. 6, D-12207 Berlin, Germany[1]; Institut für Pharmakologie, Charité, Universitätsmedizin Berlin, Campus Benjamin Franklin, D-14195 Berlin, Germany[2]; Heinrich-Pette-Institut für Experimentelle Virologie und Immunologie, D-20251 Hamburg, Germany[3]; Institut für Neuropathologie, Georg-August-Universität Göttingen, D-37075 Göttingen, Germany[4]; Institut für Pathologie, Universität Bonn, D-53127 Bonn, Germany[5]; and Weatherall Institute of Molecular Medicine, Cancer Research UK Signalling Group, University of Oxford, Oxford OX3 9DS, United Kingdom[6]

Received 22 August 2006/Returned for modification 12 October 2006/Accepted 3 April 2007

Posttranslational modification by ubiquitin controls multiple cellular functions and is counteracted by the activities of deubiquitinating enzymes. UBPy (USP8) is a growth-regulated ubiquitin isopeptidase that interacts with the HRS-STAM complex. Using Cre-loxP-mediated gene targeting in mice, we show that lack of UBPy results in embryonic lethality, whereas its conditional inactivation in adults causes fatal liver failure. The defect is accompanied by a strong reduction or absence of several growth factor receptor tyrosine kinases (RTKs), like epidermal growth factor receptor, hepatocyte growth factor receptor (c-met), and ERBB3. UBPy-deficient cells exhibit aberrantly enlarged early endosomes colocalizing with enhanced ubiquitination and have reduced levels of HRS and STAM2. Congruently immortalized cells gradually stop proliferation upon induced deletion of UBPy. These results unveil a central and nonredundant role of UBPy in growth regulation, endosomal sorting, and the control of RTKs in vivo.

Posttranslational modification of proteins by mono- or polyubiquitination represents a central mechanism for modulating a wide range of cellular functions, like protein stability, intracellular transport, protein interactions, and transcriptional activity. Ubiquitin is covalently bound to substrates by the activity of E1, E2, and E3 conjugating enzymes (17, 44, 53). Analogous to other posttranslational modifications, ubiquitination is a reversible process counteracted by deubiquitinating enzymes (DUBs), which cleave the isopeptide linkage between the protein substrate and the ubiquitin residue (14). While the processes and biological consequences of ubiquitin conjugation have been intensively studied, the role of DUBs is just beginning to emerge. Based on structural predictions, the human genome contains more than 90 putative DUBs. These fall into the subclasses of ubiquitin C-terminal hydrolases, ubiquitin-specific proteases (USPs), Machado Joseph disease protein domain proteases, ovarian tumor proteases, and JAMM motif proteases (1, 37, 42). The USPs, with more than 50 members, comprise the largest class of DUBs. Members of the USP family have been associated with the regulation of different cellular pathways. USP7 (HAUSP) regulates p53 stability by deubiquitination of p53 and Mdm2 (32, 33), USP2a was reported to regulate the stability of fatty acid synthase (12), and USP1 has been shown to deubiquitinate the monoubiquitinated proteins Fanconia anemia protein FANCD2 (41) and DNA replication processivity factor PCNA (19).

USP8 (UBPy/HUMORF8) was first described as a growth-regulated ubiquitin isopeptidase that accumulates upon growth stimulation. Protein levels of UBPy decrease, when cells undergo growth arrest by contact inhibition, suggesting a possible role in the control of mammalian-cell proliferation (40). An oncogenic fusion product of the 5′ end of phosphatidylinositol 3-kinase p85β fused to the 3′ end of UBPy, which contains the catalytic domain, was isolated from a patient with chronic myelogenous leukemia (21). Besides the catalytic domain, UBPy contains a nonclassical PX(V/I)(D/N)RXXKP Src homology 3 domain binding motif. It has been reported that via this motif, UBPy binds to Src homology 3 domains of STAM2 (23, 24) and the Grb2-like adaptor protein Mona/Gads (16). STAM2 (Hbp), together with Hrs, plays a regulatory role in endocytic trafficking of growth factor receptor complexes through early endosomes (4). Other interaction partners of UBPy that have been reported are the ubiquitin E3 ligase NRDP1 (55), the brain-specific Ras guanine nucleotide exchange factor CDC25(Mm)/Ras-GRF1 (11), and the E3 ligase GRAIL, which is crucial in the induction of CD4 T-cell anergy (50).

In the course of the work presented here, two laboratories employed RNA interference knockdown of UBPy. Controversially, they reported either accelerated degradation of epidermal growth factor receptor (EGFR) (38) or inhibition of EGFR degradation (7) upon EGF stimulation.

Here, we used conditional Cre-loxP-mediated gene targeting in mice to inactivate UBPy, and we show that lack of UBPy is lethal. It leads to growth arrest, a strong reduction of EGFR

* Corresponding author. Mailing address: Leibniz Institut für Molekulare Pharmakologie, Krahmerstr. 6, D-12207 Berlin, Germany. Phone: 493084371915. Fax: 493084371922. E-mail: knobeloch@fmp-berlin.de.

† Supplemental material for this article may be found at http://mcb.asm.org/.

▽ Published ahead of print on 23 April 2007.

and other receptor tyrosine kinases (RTKs), loss of hepatocyte growth factor-regulated tyrosine kinase substrate (HRS)-STAM complex integrity, and endosomal enlargement.

MATERIALS AND METHODS

Generation of conditional UBPy mutant mice. To generate conditional UBPy-deficient mice, a genomic DNA fragment containing exons III, IV, and V was isolated from a 129/Sv mouse genomic P1 artificial chromosome library (Resource Center of the German Human Genome Project, MPI for Molecular Genetics, Berlin, Germany). The targeting vector was constructed from a 3.5-kb PCR-amplified fragment containing exon III as 5′ homology and the adjacent SacI fragment as 3′ homology. The 5′ homology was introduced into the BamHI restriction site of the pPNTloxPneo vector. The 3′ homology encompassing exons IV and V with an additional *loxP* site, which was inserted into the EcoRV restriction site was cloned in the XhoI site of pPPNT. Embryonic stem (ES) cells (embryonic day 14.1 [E14.1]) were electroporated with NotI-linearized target vector. Selection and isolation of ES cell clones was performed as described previously (25). Two ES cell clones carrying the desired mutation were identified by Southern blotting due to the presence of an additional 5-kb BamHI/EcoRV fragment detected by probe A, which encompasses exon II. One clone was used for injection into C57BL/6 blastocysts to generate germ line chimeras. The chimeras were mated with EIIa Cre mice to excise the inserted Neo cassette as described previously (18). Mice were genotyped with the following primers: 5′-CCATGACTGCCTTTCCAGTT-3′ (primer1) and 5′-GCGATGATGAAAT TGAAATAGAT-3′ (primer2). For the wild-type (wt) allele, primers 1 and 2 amplified a 200-bp fragment, while the insertion of the *loxP* site increased the size of the PCR fragment to 260 bp. The UBPy flox/flox ($UBPy^{fl/fl}$) mice were crossed with MX-cre mice, where Cre expression can be transiently induced by the application of the interferon inducer polyinosinic-poly(C) [poly(I · C)]. To induce expression of Cre in mice carrying the myxovirus resistance gene-Cre (Mx-cre) allele, a single dose of 250 μg poly(I · C) (Sigma) was injected intraperitoneally. Mice used for analysis were on a 129OLA-C57BL/6 mixed background and were kept under standard pathogen-free conditions.

Antibodies and reagents. Recombinant murine EGF was obtained from Harbor Bio-Products. Recombinant murine beta interferon was obtained from Merck (Darmstadt, Germany); ERBB3 (C-17), c-met (SP260), and anti-β-actin (I-19) antibodies were purchased from Santa Cruz (Heidelberg; Germany); and the β-tubulin monoclonal (2-28-33) and rabbit ubiquitin antisera were from Sigma. Antibodies against polyubiquitinated and monoubiquitinated proteins (P4D1) were purchased from Santa Cruz. The antibodies against ALIX (49) and Stat1 (42) were obtained from BD Biosciences (Heidelberg, Germany). Monoclonal antibodies against TSG101 (4A10) were purchased from abcam (Cambridge, United Kingdom). Antibodies against Erk1/2, p-Erk1/2 (Thr202/Tyr204), and p-Stat1 (Tyr701) were obtained from Cell Signaling. The antibody against GAPDH (glyceraldehyde-3-phosphate dehydrogenase) (6C5) was purchased from Chemicon (Temecula, CA).

The EGFR antibody was a gift from I. Dikic (Frankfurt; Germany). The HRS and STAM2 antibodies were previously described (4, 46) and were kindly provided by H. Stenmark (Oslo, Norway). The rabbit anti-UBPy antiserum was raised against 12- and 30-amino-acid peptides from the N terminus of UBPy. Antibodies against α1 integrin and β-catenin were from P. M. Kloetzel (Berlin, Germany). Secondary horseradish peroxidase-conjugated antibodies were purchased from Santa Cruz. Antibodies for immunofluorescence were as follows: EEA1 (C15) was purchased from Santa Cruz, polyclonal cy2-or cy3-conjugated secondary antibody was purchased from Dianova (Hamburg, Germany), and Hoechst 33258 was obtained from Invitrogen (Karlsruhe, Germany).

Histological analysis. Mice were euthanized, and their organs were removed and fixed in either 4% buffered formaldehyde or Bouin's fixative. Sections were stained according to standard laboratory protocols.

EGFR immunohistochemistry. Liver tissue was fixed in 4% buffered formalin and embedded in paraffin. SC-03 (Santa Cruz Biotechnology, Santa Cruz, CA) was used for immunohistochemical analysis of EGFR expression.

Retroviral infection. The pMIEG3 plasmid (54) was obtained from D. A. Williams. Modified human estrogen receptor (ERT2) fused to the C terminus of Cre recombinase (10) was a gift from Pierre Chambon. The Cre-ERT2 sequence was inserted in the EcoRI site of the pMieg3 plasmid, resulting in a retroviral construct driving bicistronic expression of Cre-ERT2 and enhanced green fluorescent protein (GFP).

For virus production, Phoenix-gp cells were plated at a density of 3×10^6 to 5×10^6 cells per 10-cm dish. The next day, the cells were transfected by calcium precipitation with plasmids (M57) encoding Gag-Pol, the ecotropic envelope (K73), and the Cre-Ert2-MIEG3 in the presence of 25 mM chloroquine. Six to 10 h later, the medium was replaced. The supernatant, containing retroviral particles, was harvested 48 h after transfection.

For retroviral infection of murine embryonic fibroblasts (MEFs), cells were plated at a density of 1×10^6 cells per 10-cm dish 1 day prior to infection. The next day, the cells were infected with virus in the presence of Polybrene at a final concentration of 8 ng/ml; 16 h later, the medium was replaced with fresh virus supernatant for another 8 h.

Cell culture and cell lines. MEFs were isolated and cultured as described previously (43). Cells were immortalized by frequent passaging. To generate a cell line in which a UBPy deletion could be induced with 4-hydroxytamoxifen, immortalized $UBPy^{fl/fl}$ MEFs were infected with a retrovirus carrying an expression construct for Cre fused to the mutated ligand-binding domain of the human estrogen receptor (Cre-ERT2), followed by an internal ribosome entry site GFP cassette. Six days after infection, the cells were sorted for GFP expression using a FACSVantage cell sorter at the Flow Cytometry and Cell Sorting Core Facility of DRFZ (Campus Charité Mitte, Berlin, Germany). After one more week in culture, a second round of sorting was performed. To induce deletion, cells were cultured in media containing 1 μM 4-hydroxytamoxifen.

EGF stimulation. One day prior to stimulation, 3.5×10^5 MEFs were plated in a 6-cm dish and starved for 16 h in medium containing 0.1% serum. The next day, the cells were stimulated with 100 ng/ml EGF for the indicated time. The cells were washed with ice-cold phosphate-buffered saline (PBS) and subsequently lysed in 120 μl sodium dodecyl sulfate (SDS) buffer as described below.

Determination of MEF growth. To determine cell growth, 0.8×10^6 to 1×10^6 MEFs were plated in triplicate on 10-cm dishes; 2 to 3 days later, the total number of cells was determined, and 0.8×10^6 to 1×10^6 cells were replated to prevent contact inhibition. The accumulated total cell numbers were calculated. Bromodeoxyuridine (BrdU) incorporation in MEFs was performed according to the manufacturer's instructions (Roche). The cells were counterstained with Hoechst 33258 and analyzed with a fluorescence microscope.

Immunofluorescence. For immunofluorescence studies, cells were washed twice with ice-cold KRH buffer (130 mM NaCl, 4.7 mM KCl, 2.5 mM $CaCl_2$, 1.2 mM KH_2PO_4, 1.2 mM $MgSO_4$, 5.5 mM glucose, 10 mM HEPES) and fixed with paraformaldehyde (2.5% [wt/vol] in PBS, pH 7.4). The cells were permeabilized with 0.1% Triton X-100 in PBS for 3 min. Nonspecific binding of antibodies was blocked with 0.5% bovine serum albumin in PBS prior to incubation with primary antibody. Polyclonal cy2- or cy3-conjugated secondary antibody (Dianova, Hamburg, Germany) was used for detection. The cells were mounted with Immumount (Thermo Electron, Dreieich, Germany).

The samples were analyzed at a λ_{exc} of 488 nm and λ_{em} of >515 nm for cy2 staining and a λ_{exc} of 525 and λ_{em} of >568 nm for cy3 staining with the LSM 410 inverted laser scanning microscope (Carl Zeiss, Jena, Germany).

Protein extracts and immunoblotting. Cells in 6-cm dishes were lysed with SDS buffer (7% SDS, 0.125 M Tris-HCl, pH 6.8) or RIPA buffer (50 mM Tris-HCl, pH 7.4, 1% NP-40, 0.25% sodium deoxycholate, 50 mM NaCl, 10 mM EDTA) containing protease inhibitors (Roche), and the lysates were sonified and centrifuged. Protein was separated on SDS-polyacrylamide gels, and Western blots were incubated with primary antibodies according to the manufacturer's protocol. Tissues were directly homogenized in SDS buffer.

Northern blot analysis. Total RNA was extracted with Tri-reagent (Sigma); 15 μg RNA per lane was loaded on a 1.2% agarose gel containing 1% formaldehyde and blotted. Probes were radioactively labeled with Rediprime (Amersham) and hybridized using Express-Hyb-Solution (Clontech) according to the manufacturer's protocol.

cDNA probes were amplified using the following primers: EGFR, 5′-TGC CCA TGC GGA ACT TAC AGG A-3′ (upper strand) and 5′-GTT TCG GGG GCA CTT CTT CAC AC-3′ (lower strand); GAPDH, 5′-GGG GTG AGG CCG GTG CTG AGT AT-3′ (upper strand) and 5′-CAT TGG GGG TAG GAA CAC GGA AGG-3′ (lower strand).

TUNEL stains. The terminal deoxynucleotidyltransferase-mediated dUTP-biotin nick end labeling (TUNEL) assay of liver sections and fixed cells was performed according to the manufacturer's instructions (Roche). Apoptotic cells were analyzed with a fluorescence microscope.

Blood plasma analysis. Animals were sacrificed, and blood was collected by cardiac puncture. Heparin plasma was separated, and samples were analyzed as described previously (49).

Analysis of proteasomal activity. The chymotryptic activity of the proteasome was assessed in liver lysates or cell lysates of MEFs using the synthetic peptide substrate Suc-Leu-Leu-Val-Tyr linked to the fluorometric reporter AMC. Cells were lysed in TSDG buffer (10 mM Tris-HCl, pH 7.0, 25 mM KCl, 10 mM NaCl, 1.1 mM $MgCl_2$, 0.1 mM EDTA, 1 mM dithiothreitol, 1 mM NaN_3, 10% glycerol, 2 mM ATP) containing protease inhibitors (Roche). After centrifugation, the

supernatants were used for determination of the protein concentration and enzymatic activity. The lysates were incubated for 30 min at 37°C in TSDG buffer containing 0.2 mM Suc-Leu-Leu-Val-Tyr AMC. AMC hydrolysis was quantitated in a BioTek FLx800 plate reader using 360-nm excitation and 460-nm emission wavelengths. Enzymatic activity was normalized to the protein concentration.

Electron microscopy. For electron microscopy, ultrathin sections of glutaraldehyde-fixed wt and ΔUBPy cells were treated with uranyl acetate and lead citrate. Electron micrographs were analyzed using the analySIS Docu System (Soft Imaging System GmbH, Germany).

Statistical analysis. Values are given as means ± standard errors of the mean. Statistical differences were determined using Student's *t* test.

RESULTS

Embryonic lethality in mice with targeted deletion of UBPy. To analyze the function and biological relevance of UBPy in the context of the whole organism, we generated mice that allowed the conditional inactivation of UBPy using Cre-loxP-mediated gene targeting. As shown in Fig. 1A, after homologous recombination of the target vector and subsequent deletion of the neomycin resistance cassette, exon IV was flanked by *loxP* sites. Upon *cre*-induced recombination, exon IV can be excised, causing a frameshift in the potentially remaining truncated mRNA, leading to premature translational termination. Successful recombination of the target vector was monitored by the appearance of a 5-kb fragment, detected with probe A due to the insertion of an additional BamHI site in the UBPy gene locus (Fig. 1B). Mice were produced from these ES cells, and the neomycin resistance cassette was removed as described in Materials and Methods. Correct mutation in $UBPy^{fl/fl}$ mice was further validated by the amplification and sequencing of a 4.2-kb fragment with primers P1 (located in the distal *loxP* site) and P2 (located adjacent to the 3′ homology of the target vector) (Fig. 1C). After the mice were mated to EIIa-*cre* mice (30), UBPy was deleted from one allele and heterozygotes ($UBPy^{+/-}$) were interbred. Offspring from these matings yielded 13 $UBPy^{+/+}$ (27.7%) and 34 $UBPy^{+/-}$ (72.3%) animals, but no $UBPy^{-/-}$ mice, indicating that the lack of UBPy results in embryonic lethality.

To determine the phenotype of the mutants, heterozygote mice were mated and embryos recovered from pregnant animals were photographed and genotyped. At E9.5, embryos of all genotypes could be recovered. However, mutant animals were dramatically retarded in size and appeared grossly disorganized (Fig. 1E). It seemed that the mutant embryos did not initiate ventral folding, a prerequisite for heart formation, and they seemed to suffer from significant growth retardation. The morphology of the mutant embryo was reminiscent of the Hrs knockout (27), which displays defects in ventral folding at E8.0. However, in addition, the UBPy mutant was dramatically growth retarded, indicating a general defect in embryonic development rather than affecting a specific structure.

Severe liver failure and death upon induced deletion of UBPy in adult mice. To induce inactivation of UBPy in adult mice, animals with the floxed UBPy gene ($UBPy^{fl/fl}$) were bred with MX-Cre transgenic mice (29). In animals that carry the MX-Cre transgene together with the homozygous UBPy-flox allele ($UBPy^{fl/fl}$ MX-Cre), inactivation of UBPy (ΔUBPy) was achieved by administration of poly(I · C). The efficient deletion of the targeted DNA sequence was monitored by UBPy protein levels in the liver, which were undetectable 4 to 6 days after induction of Cre (Fig. 1D).

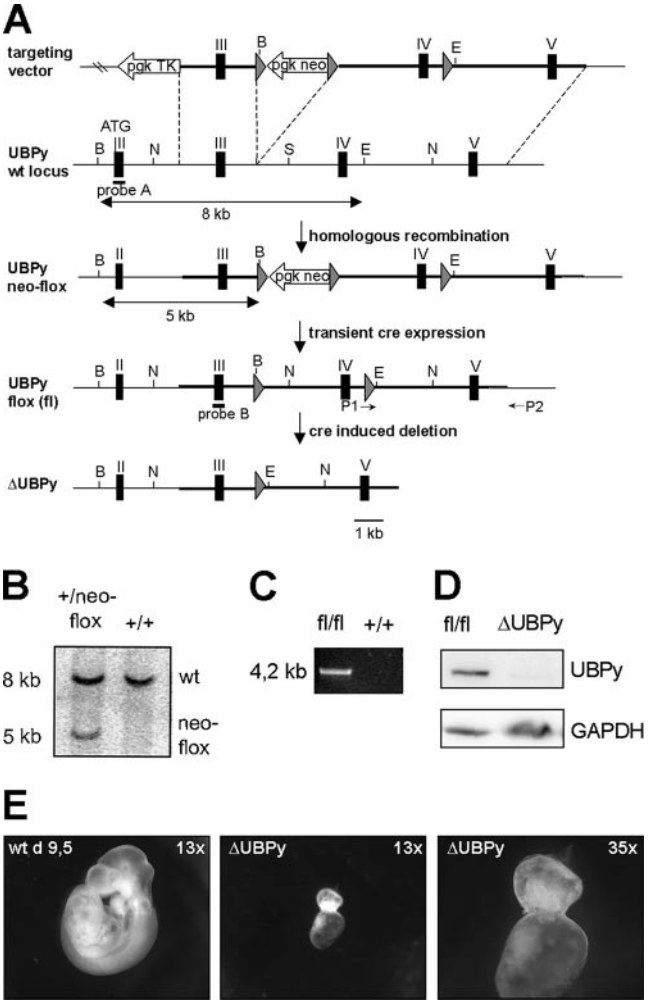

FIG. 1. Conditional mutagenesis of the UBPy gene. (A) Targeting strategy. The solid boxes indicate exons. The orientations of the *pgk neo* and *pgk*-TK genes are indicated by arrows. *loxP* sites are depicted as triangles. Restriction enzymes are as follows: N, NcoI; B, BamHI; E, EcoRV; and S, SacI. (B) Southern blot of an ES cell clone upon homologous recombination with the target vector. Genomic DNA was digested with BamHI plus EcoRV, blotted, and hybridized using external probe A. As indicated in the targeting strategy, after homologous recombination of the target vector, an additional BamHI site is inserted in the genome. Thus, probe A detects an additional 5-kb fragment in a clone that has been successfully mutated. (C) Correct 3′ integration of the target vector. PCR was performed on genomic DNA from $UBPy^{fl/fl}$ mice and wt controls. Amplification of a 4.2-kb fragment with primers P1 an P2 was diagnostic for the mutated allele. (D) Immunoblot of MX-Cre-induced deletion of UBPy in the liver. MX-Cre $UBPy^{fl/fl}$ mice were stimulated with poly(I · C) as described in Materials and Methods to induce Cre expression. After 6 days, protein expression was analyzed by Western blotting using antiserum against UBPy. (E) Morphology of UBPy-deficient embryos (ΔUBPy). Embryos were isolated from heterozygous matings 9.5 days postcoitus, photographed, and genotyped.

Mutant mice with the induced deletion of UBPy (ΔUBPy mice) died 4 to 6 days after the administration of poly(I · C), demonstrating an essential, nonredundant function of UBPy in vivo (Fig. 2A). The loss of UBPy was accompanied by the development of a severe icterus in moribund mice. As demonstrated in Fig. 2B, the hyperbilirubinemia with dramatically

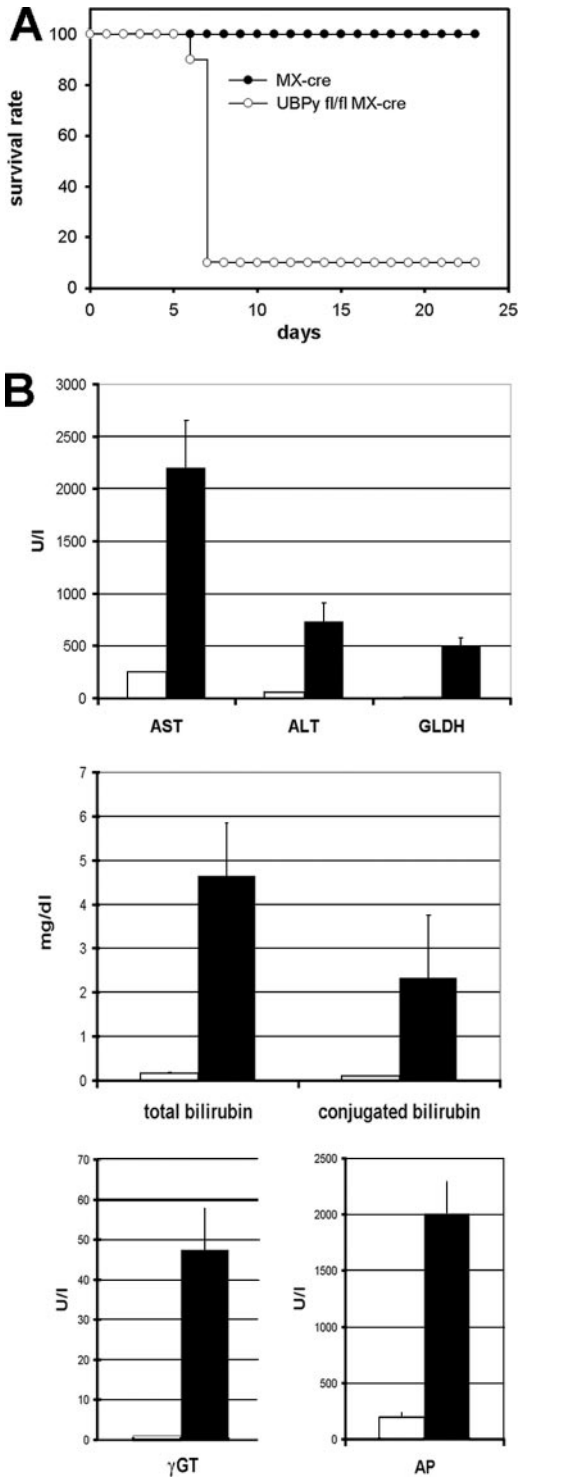

FIG. 2. Deletion of UBPy in adult mice leads to death caused by disturbed liver function. (A) Survival rates of mice upon induction of UBPy deletion. Cre-mediated deletion of UBPy in UBPy$^{fl/fl}$ MX-Cre and MX-Cre mice (10 per group) was induced with poly(I · C) as described in Materials and Methods. (B) Analysis of liver parameters in ΔUBPy mice. Seven days after poly(I · C) induction, plasmas of 10 UBPY$^{+/+}$ MX-Cre^{+} controls (open bars) and 12 UBPY$^{fl/fl}$ MX-Cre^{+} (ΔUBPy; solid bars) mice were analyzed. The liver-specific enzymes were as follows: AST, aspartate transaminase; ALT, alanine transaminase; GLDH, glutaraldehyde-dehydrogenase; γGT, gamma-glutamyl-transferase; AP, alkaline-phosphatase. The error bars indicate standard errors of the mean.

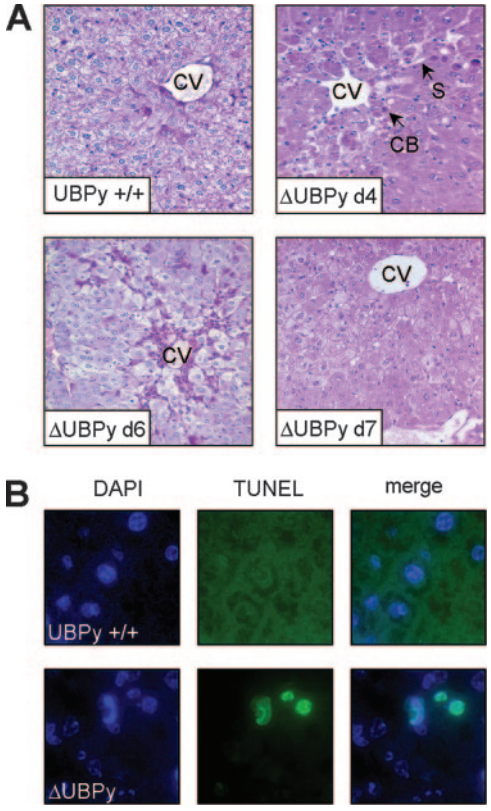

FIG. 3. Lack of UBPy causes progressive liver injury. (A) Morphological analysis of liver sections. Paraffin sections were stained with hematoxylin and eosin. Abbreviations are as follows: CV, central vene; CB, Councilman bodies; S, liver sinosoid. (B) Enhanced apoptosis in hepatocytes lacking UBPy. TUNEL staining was performed 4 days after poly(I · C) induced UBPy deletion.

increased concentrations of both conjugated and total bilirubin indicates severely disturbed liver function. Liver injury in mice lacking UBPy was further confirmed by strongly increased serum concentrations of aspartate transaminase and alanine transaminase and was accompanied by higher alkaline phosphatase and gamma-glutamyl-transferase, as well as glutaraldehyde dehydrogenase levels (Fig. 2B). Histological analysis of liver sections revealed that pathological changes started 4 days after the administration of poly(I · C), as manifested by apoptotic hepatocytes (Councilman bodies) around the central vein (Fig. 3A). On day 4, extended sinoids and apoptotic figures were observed. Cells around the portal field, which represent a more immature form of hepatocytes, showed swelling and were vacuolized. Starting from day 6, apoptotic figures and ubiquitous degeneration of hepatocytes were spread over all zones of hepatic lobules, with lytic necrosis visible on day 7 after poly(I · C) injection. Apoptotic hepatocytes in ΔUBPy mice were visualized by TUNEL staining (Fig. 3B). Together, the data provide strong evidence that the death of ΔUBPy mice is caused by a severe liver failure.

Induced deletion of UBPy in an immortalized MEF cell line leads to growth arrest. To further dissect the consequences of UBPy deletion on a cellular level and to evaluate the molecular mechanisms, we employed a model system that allowed inducible inactivation of UBPy in cell culture. Therefore, a tamox-

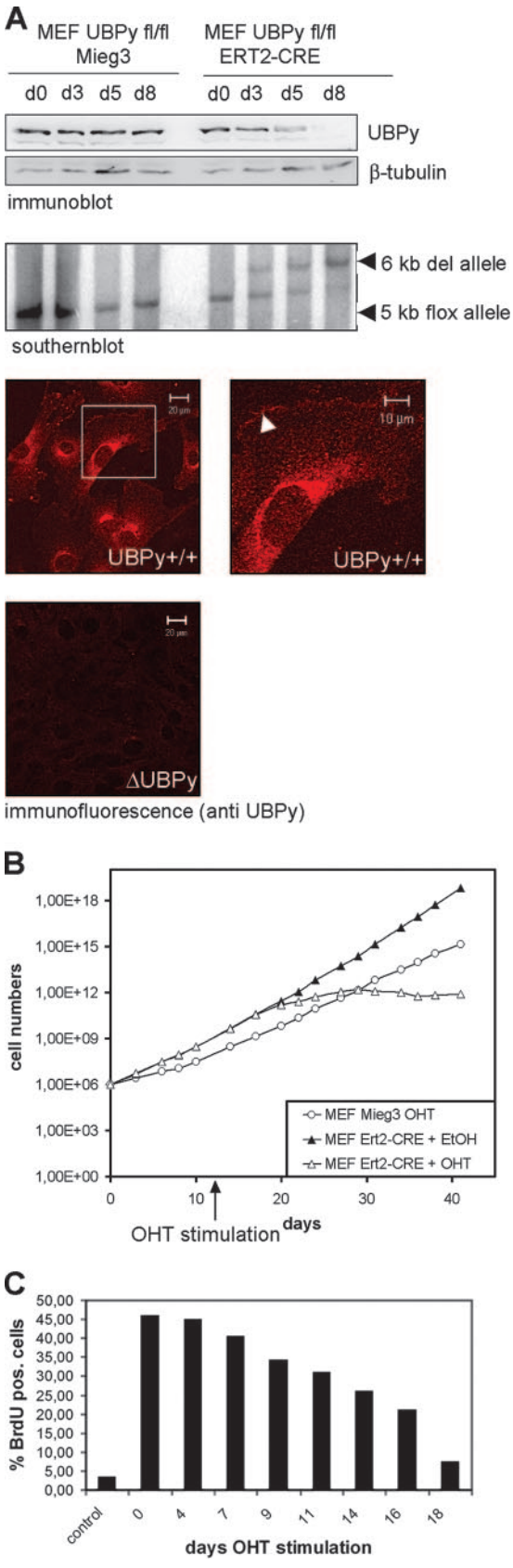

FIG. 4. Impaired proliferation and growth arrest of immortalized cells upon deletion of UBPy. (A) A MEF-derived immortalized cell line with inducible deletion via Cre-ERT2/tamoxifen (UBPy$^{fl/fl}$ ERT2 *cre*) was established as described in Materials and Methods. To induce deletion, tamoxifen was added to the cell culture media for the indicated periods. Complete deletion of UBPy was achieved after 4 to 5 days, as assessed by immunoblotting, Southern blotting, and immunofluorescence. To monitor deletion by Southern analysis, genomic DNA was digested with NcoI. As depicted in Fig. 1, *cre*-mediated deletion eliminates an NcoI site from the genome. Thus, probe B detects a 5-kb fragment on the floxed allele and a 6-kb band upon *cre*-mediated deletion. The enlarged image of the boxed area (middle right) shows subcellular localization of UBPy upon immunofluorescence staining against UBPy. Membrane staining is indicated by an arrowhead. d, day. (B) Growth properties of cells with or without deletion of UBPy. Cumulative cell numbers were determined as described in Materials and Methods. The solid triangles represent untreated UBPy$^{fl/fl}$ ERT2 Cre cells. Tamoxifen (OHT) was added at the indicated time point to induce deletion (open triangles). To exclude any influence of tamoxifen on cell proliferation, UBPy$^{fl/fl}$ cells stably carrying a MIEG3 retrovirus (UBPy$^{fl/fl}$ MIEG3; open circles) were treated with tamoxifen as a control. EtOH, ethanol. (C) BrdU incorporation in immortalized embryonic fibroblasts upon UBPy deletion was determined at the indicated time points as described in Materials and Methods. Mitomycin C-treated cells served as a control. pos., positive.

ifen-inducible recombination system was used (9). An immortalized embryonic fibroblast cell line derived from UBPy$^{fl/fl}$ animals was infected with a retrovirus carrying Cre fused to the mutated ligand-binding domain of the human estrogen receptor (Cre-ERT2), as described in Materials and Methods. Upon administration of tamoxifen to UBPy$^{fl/fl}$ cells stably expressing Cre-ERT2, Cre translocates to the nucleus and induces the deletion of UBPy (ΔUBPy). Using this system, UBPy was completely deleted 4 to 6 days after tamoxifen induction, as shown by Southern, Western, and immune fluorescence analyses (Fig. 4A). As the polyclonal antisera used for immunfluorescence exhibited no background staining in ΔUBPy cells, we were able to trace the subcellular localization of endogenous UBPy to a perinuclear region and to the cell membrane (Fig. 4A).

Since UBPy was linked to growth regulation (40), we compared the proliferative capacities of cells with and without induced deletion of UBPy. As shown in Fig. 4B, cells completely stopped growing 6 to 8 days after deletion of UBPy. In concordance with impaired proliferation, BrdU incorporation in ΔUBPy cells was severely reduced (Fig. 4C). In contrast to the situation in hepatocytes, this was not accompanied by reduced cell viability or enhanced apoptosis, as cell numbers did not drop for a period of more than 10 days after growth arrest and the percentage of ΔUBPy cells staining positive in a TUNEL assay was similar to that of undeleted cells (see Fig. S1 in the supplemental material). The results show that UBPy plays a central role in cellular proliferation and that its inactivation is sufficient to induce growth arrest.

Decreased protein levels of RTKs c-met, EGFR, and ERBB3 in UBPy-deficient mice. The loss of proliferative capacity of cells lacking UBPy would be compatible with an impairment of stimulation by growth factors. Therefore, we analyzed the protein levels of EGFR as a prototype RTK in UBPy$^{+/+}$ and ΔUBPy cells. As shown in Fig. 5A, the loss of UBPy was followed by a strong reduction of EGFR protein levels. In concordance with this result, EGF signaling was also impaired, as appraised from the phosphorylation of Erk1/2 (Fig. 5B). In

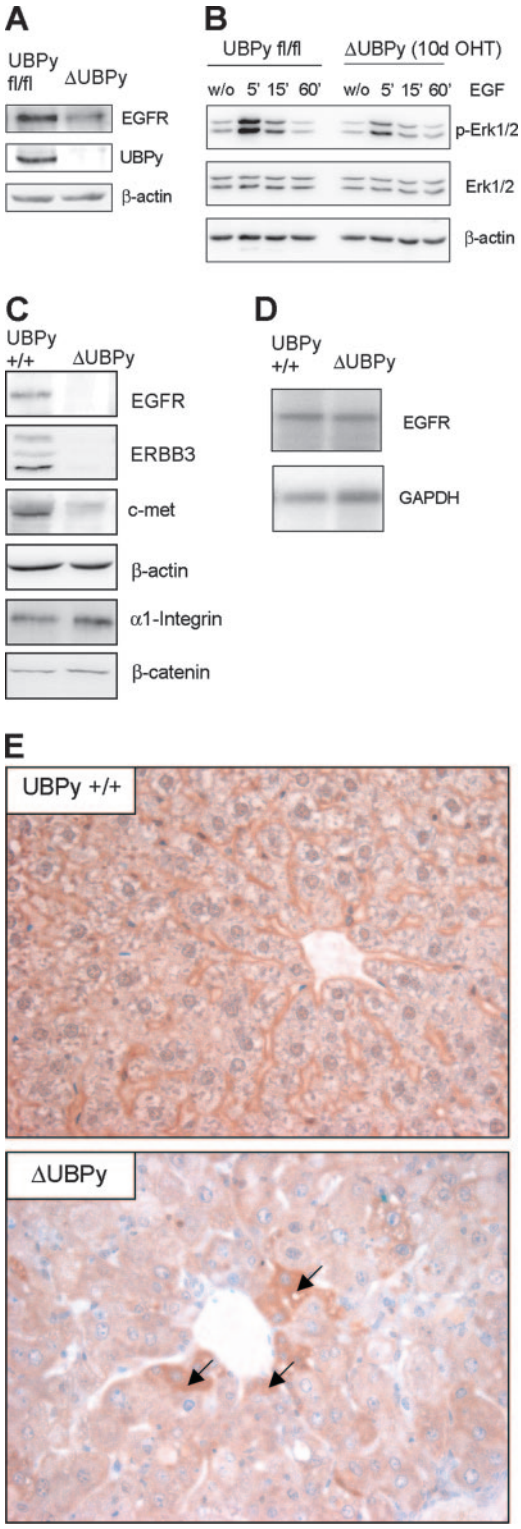

FIG. 5. Lack of UBPy results in strongly reduced protein levels of the RTKs EGFR, ERBB3, and c-met. (A) Immunoblot analysis of EGFR. UBPy$^{fl/fl}$ ERT2 Cre cells were treated with tamoxifen for 10 days to induce deletion of UBPy (ΔUBPy). Untreated cells (fl/fl) were used as controls. Immunoblots from cell extracts were incubated with the indicated antibodies as described in Materials and Methods. (B) Phosphorylation of ERK1/2 upon stimulation with EGF. UBPy$^{fl/fl}$ ERT2 Cre cells were treated with tamoxifen for 10 days to induce deletion of UBPy (ΔUBPy). Cells with or without induced deletion of UBPy were starved for 16 h. Subsequently, the cells were stimulated with 100 ng/ml EGF as described in Materials and Methods. Cells were lysed at the indicated time points, and phosphorylation of ERK1/2 as a readout for EGF stimulation was analyzed by immunoblotting using a pERK1/2-specific antibody. Equal loading was confirmed by reprobing the blot with either antiactin or anti-ERK antiserum. (C) RTK expression in liver extracts. MX-Cre UBPy$^{fl/fl}$ mice were stimulated with poly(I · C) as described in Materials and Methods to induce Cre-mediated deletion of UBPy (ΔUBPy). After 6 days, protein expression was analyzed by immunoblotting with antisera specific for the indicated proteins. (D) mRNA expression of EGFR in the liver. Total RNA was extracted from the livers of UBPy$^{+/+}$ and ΔUBPy mice. A Northern blot was hybridized as described in Materials and Methods using a probe specific for the EGFR. (E) Localization of EGFR in liver sections. Liver sections were immunohistochemically stained with antisera specific for EGFR, as described in Materials and Methods. The arrows indicate cells exhibiting cytoplasmic EGFR localization.

contrast, the lack of UBPy did not affect STAT-1 phosphorylation upon alpha/beta interferon induction (see Fig. S2 in the supplemental material), showing that the capability to transduce extracellular signals was not globally disturbed.

The complete inhibition of proliferation observed in UBPy-deficient cells could hardly be explained by the absence of EGFR signaling alone. Several other growth factors present in the media should be sufficient to maintain at least a certain extent of proliferation. Therefore, and to evaluate whether the lack of UBPy also affects protein levels of RTKs in the context of the whole organism, liver extracts from UBPy$^{+/+}$ and ΔUBPy mice were tested by immunoblotting. As shown in Fig. 5C, c-met, EGFR, and ERBB3 protein levels in ΔUBPy livers were strongly decreased (c-met) or even below detection levels (EGFR and ERBB3), whereas levels of α-integrin and β-catenin were unchanged.

To determine whether the lack of UBPy causes the decrease of RTK expression on the RNA or protein level, RNA expression of EGFR in the liver was analyzed. EGFR mRNA levels did not differ significantly between UBPy$^{+/+}$ and ΔUBPy animals (Fig. 5D), demonstrating that the lack of EGFR protein expression is based on a disturbance of posttranscriptional regulation.

It is well documented that upon ligand stimulation RTKs undergo ubiquitin-mediated internalization leading to degradation via the endosomal-lysosomal pathway (13, 39). Immunohistochemical analysis of liver sections revealed that in most hepatocytes of ΔUBPy mice, EGFR is no longer detectable, confirming the results from Western analysis. Remarkably, in the few ΔUBPy hepatocytes in which EGFR was still detectable, the receptor was no longer localized to the cell membrane but exhibited a cytoplasmic staining, providing evidence that enhanced internalization followed by lysosomal degradation is the cause of the severe reduction of RTK protein levels (Fig. 5E). The results show a critical role of UBPy in cellular proliferation pursued via the control of RTK stability.

Lack of UBPy causes endosomal enlargement, accumulation of multivesicular bodies (MVBs), and destabilization of the HRS-STAM complex. Ubiquitinated membrane receptors are internalized by ubiquitin-mediated endocytosis and first locate to early endosomes, which upon invagination of their membranes mature to MVBs, which subsequently fuse to lyso-

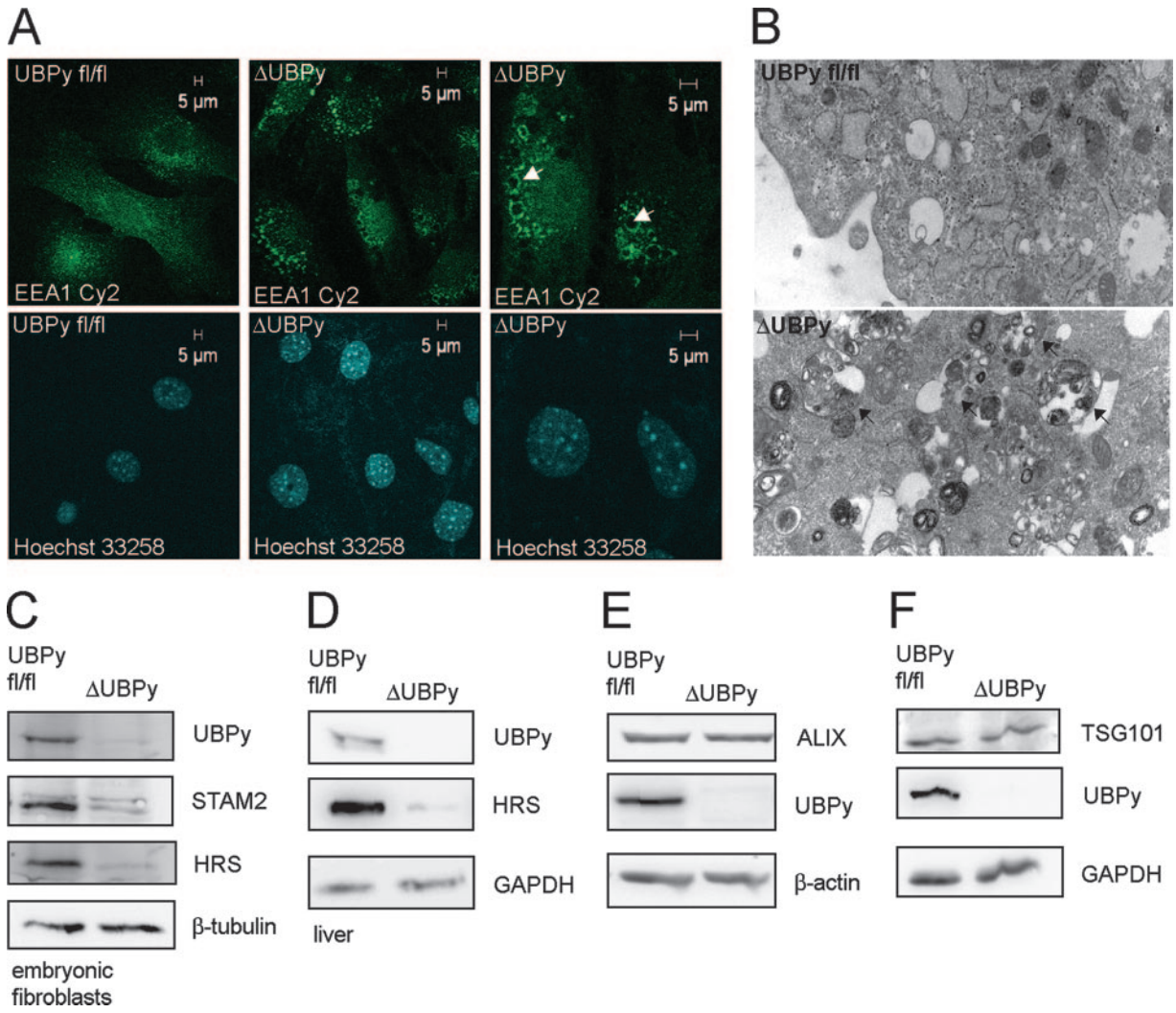

FIG. 6. Enlargement of early endosomes, accumulation of MVBs, and reduction of HRS and STAM2 in cells lacking UBPy. (A) Enlarged early endosomes in cells lacking UBPy. UBPy$^{fl/fl}$ ERT2 Cre cells were cultured in the presence of tamoxifen for 10 days to induce deletion of UBPy (ΔUBPy). Subsequently, the cells were fixed and stained with antibodies against the early endosomal marker EEA1 and cy2-conjugated secondary antibody. The cells were analyzed by confocal laser microscopy as described in Materials and Methods. Cell nuclei were counterstained with Hoechst 33258. The arrowheads indicate enlarged early endosomes. (B) Ultrastructural examination of cells upon induced deletion of UBPy. UBPy$^{fl/fl}$ ERT2 Cre cells were cultured in the presence of tamoxifen for 10 days to induce deletion of UBPy (ΔUBPy). Subsequently, the cells were analyzed by electron microscopy as described in Materials and Methods. The arrows indicate MVBs. (C) Induced inactivation of UBPy in the MEF-derived cell line correlates with decreased HRS and STAM2 protein levels. UBPy$^{fl/fl}$ ERT2 Cre cells were cultured in the presence of tamoxifen for 10 days to induce deletion of UBPy (ΔUBPy). Untreated cells (UBPy$^{fl/fl}$) were used as controls. Protein extracts were analyzed by immunoblotting using antisera specific for the indicated proteins. (D) Decreased protein levels of HRS and STAM2 in liver extracts from ΔUBPy mice. UBPy$^{fl/fl}$ MX-Cre mice were stimulated with poly(I · C) as described in Materials and Methods to induce *cre*-mediated deletion of UBPy (ΔUBPy). After 6 days, protein extracts were prepared from the liver and analyzed by immunoblotting with antisera specific for the indicated proteins. (E and F) Unaltered expression of ALIX and TSG101. UBPy$^{fl/fl}$ ERT2 Cre cells were cultured in the presence of tamoxifen for 9 days to induce deletion of UBPy (ΔUBPy). Protein extracts were analyzed by immunoblotting using antisera specific for the indicated proteins.

somes. When UBPy-deficient cells were stained with the early endosomal marker EEA1, a drastic enlargement of early endosomes was detected (Fig. 6A). In addition, ultrastructural examination of ΔUBPy cells by electron microscopy showed an accumulation of MVBs (Fig. 6B) and exhibited enlarged vacuole-like structures already visible by light microscopy (see Fig. S3 in the supplemental material), indicating enhanced activity of the endosomal pathway. A key factor involved in the endosomal sorting process is HRS. HRS-deficient fibroblasts also exhibit enlarged endosomes and show enlarged vacuole-like structures, like UBPy-deficient MEFs (27). In addition, HRS forms a complex with STAM2 (51), which was described as an interaction partner of UBPy (24). Thus, we asked whether UBPy might stabilize this complex. Protein expression levels of HRS and STAM2 in cells before and after tamoxifen-induced deletion of UBPy are shown in Fig. 6C. The absence of UBPy led to a strong reduction, or even absence, of HRS and STAM2 protein levels, indicating that UBPy is essential for the stability of the HRS-STAM complex.

Strongly decreased HRS protein levels were also detected in

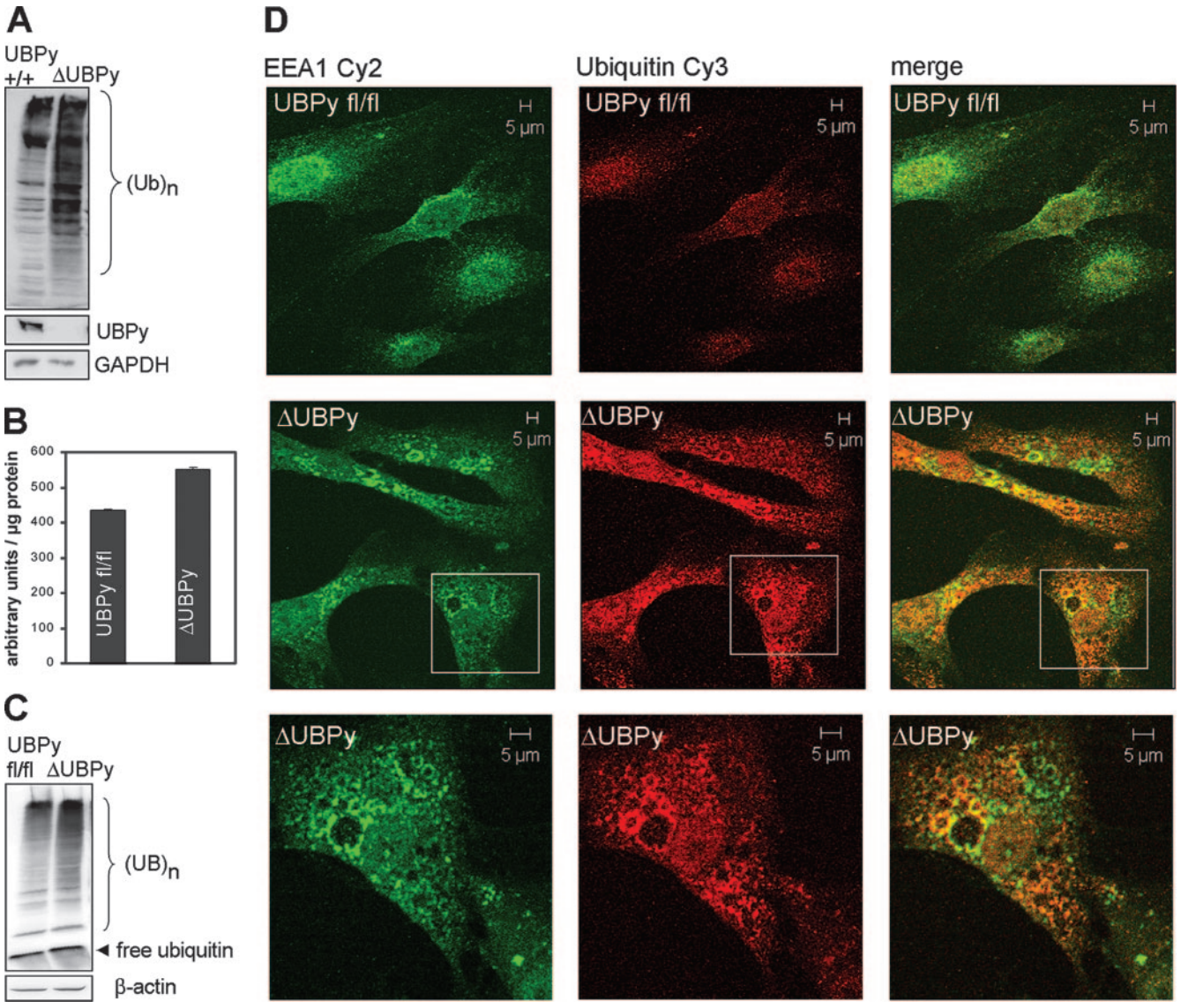

FIG. 7. Enhanced protein ubiquitination in ΔUBPy cells colocalizes with enlarged early endosomes. (A) Enhanced ubiquitination in mice lacking UBPy. $UBPy^{fl/fl}$ MX-Cre mice were stimulated with poly(I · C) as described in Materials and Methods to induce *cre*-mediated deletion of UBPy (ΔUBPy). After 6 days, protein extracts were prepared from the liver, separated on 7% SDS-polyacrylamide gel electrophoresis (PAGE), and analyzed by immunoblotting with antiubiquitin antibody to detect ubiquitin-conjugated substrates $[(UB)_n]$. (B) Lack of UBPy does not impair proteasomal activity. $UBPy^{fl/fl}$ MX-Cre mice were stimulated with poly(I · C) for 6 days as described in Materials and Methods. Proteasomal activity was tested using liver extracts as described in Materials and Methods. (C) Deletion of UBPy does not affect ubiquitin chain disassembly. $UBPy^{fl/fl}$ ERT2 Cre cells were treated with tamoxifen for 10 days to induce deletion of UBPy (ΔUBPy). Protein extracts were separated on a 5 to 20% gradient SDS-PAGE, and immunoblots were incubated with ubiquitin-specific antisera to detect free and conjugated ubiquitin. (D) Enhanced ubiquitination colocalizes with enlarged endosomes. $UBPy^{fl/fl}$ ERT2 Cre cells were cultured in the presence of tamoxifen for 10 days to induce deletion of UBPy (ΔUBPy). Subsequently, the cells were fixed and stained with antibodies against the early endosomal marker EEA1, conjugated ubiquitin, and cy2-conjugated (EEA1) or cy3-conjugated (ubiquitin) secondary antibodies. The cells were analyzed by confocal laser microscopy as described in Materials and Methods.

vivo, as seen from the analysis of liver extracts of ΔUBPy mice (Fig. 6D). In contrast, levels of the UIM-containing proteins ALIX (36) and TSG101 (5, 31), which are also associated with endosomal sorting processes, were not affected by the loss of UBPy (Fig. 6E and F). These data provide strong evidence for a functional role of UBPy in endosomal sorting pursued by stabilizing the HRS-STAM complex.

ΔUBPy cells show accumulation of ubiquitinated substrates colocalizing with enlarged early endosomes. Consistent with the function of UBPy as a DUB, enhanced levels of ubiquitinated substrates were detected in liver extracts from ΔUBPy mice (Fig. 7A). This could be explained either by a lack of deconjugation of Ub chains from distinct substrates or, alternatively, by impaired proteasomal activity resulting in the accumulation of ubiquitinated proteins. Thus, we tested the proteasomal activity in liver extracts from $UBPy^{+/+}$ and UBPy-deficient mice. As shown in Fig. 7B, even slightly higher proteasomal activity was detected in ΔUBPy extracts, suggesting

that proteasomal inhibition is not the cause of the enhanced ubiquitination levels. It has been speculated that UBPy might be the functional homologue of yeast DOA4, which has been shown to be essential for the regeneration of ubiquitin from polyubiquitin chains (3). To examine the impact of the lack of UBPy on polyubiquitin chain disassembly, we compared the levels of free ubiquitin in wt and UBPy-deficient cells. As shown in Fig. 7C, both types of cells showed the same amount of free ubiquitin, demonstrating that UBPy is not necessary to restore the pool of free ubiquitin and does not exert a function similar to that of DOA4 in this respect. The results suggest that UBPy directly counteracts ubiquitination on distinct substrates.

In order to determine whether the enhanced ubiquitinated substrates were uniformly distributed over the cell or were attributed to defined subcellular structures, cells were stained with an antibody recognizing conjugated ubiquitin. As shown in Fig. 7D, enhanced ubiquitination colocalized with the enlarged early endosomes, providing evidence that the lack of UBPy results in aberrant ubiquitination of substrates that are targeted to the endosomal lysosomal degradation pathway. Alternatively, UBPy might exert its deubiquitinating activity exclusively on early endosomal structures.

DISCUSSION

While considerable progress has been made in defining the functional properties of different USPs using in vitro and cell culture systems, their physiological relevance in the context of the whole organism is only poorly understood. Recently, mice deficient in CYLD, a USP that is altered in patients with familial cylindromatosis, were generated. Contrary to results from transfection experiments, which suggested a negative regulatory function of CYLD on NF-κB activation (8, 28, 52), bone marrow-derived macrophages from wt and CYLD$^{-/-}$ animals did not differ in innate immune receptor signaling. Analysis of these mice instead demonstrated an essential role for CYLD in T-cell development (47), underlining the necessity of mouse models to evaluate functional properties of DUBs in vivo.

It was a matter of debate whether and to what extent different DUBs might have redundant functions (2). UBPy-deficient animals are embryonic lethal, and induced inactivation in adulthood causes fatal liver failure. This clearly shows that lack of UBPy cannot be compensated for by other DUB family members in vivo. Embryonic lethality might at least partially be attributed to the lack of HRS, as HRS- deficient animals also exhibited embryonic lethality caused by ventral-folding defects. However, while HRS-deficient embryos were often as large as wt controls and even had beating hearts by day 9.5 (27), UBPy$^{-/-}$ animals were extremely developmentally retarded and exhibited completely disorganized morphology at that time point. This shows that besides the stabilization of HRS, UBPy is essential for embryonic growth. The observation that UBPy-deficient fibroblasts underwent growth arrest further supports an essential role of UBPy in the control of cellular proliferation. MX-Cre-mediated deletion of floxed genes in general leads to the fastest and most efficient deletion in the liver (29), which most likely explains why the phenotype manifests in that organ, although UBPy is also expressed in other cell types. The strong liver phenotype demonstrates that, besides a role in proliferation, UBPy is also essential in quiescent cells, like hepatocytes. As loss of UBPy in hepatocytes caused apoptosis and cell death while embryonic fibroblasts did not exhibit enhanced apoptosis, functional differences of UBPy in different cell types or in proliferating versus nonproliferating cells apparently exist.

Pathology in the liver can most likely be attributed to the combined effects of disturbed endosomal function, loss of several RTKs, and disturbed liver regeneration caused by the absence of c-met, which has been shown to be essential for this process (6, 20). Due to the severity of the phenotype in the liver and early death, cell-type-specific inactivation will be necessary to define the physiological relevance in other organs or cell types.

We have shown that in vivo UBPy is essential to maintain proper protein levels of RTKs, like EGFR, c-met, and ERBB3, and thus reduced growth factor stimulation might at least partially contribute to the growth arrest in UBPy$^{-/-}$ cells. As a common feature of several RTKs, ligand binding induces ubiquitination as a signal to internalize the receptor via endocytosis (15). Although the detailed mechanisms leading to the reduction or even absence of several RTKs in UBPy-deficient mice need to be defined, the observed cytoplasmic localization of EGFR in UBPy-deficient hepatocytes strongly suggests that, due to the loss of UBPy, RTKs undergo enhanced internalization followed by lysosomal degradation. The results are compatible with a model in which UBPy counteracts ubiquitination of RTKs or components of the endocytic machinery and thus regulates thresholds for the internalization of growth factor receptors.

The observed accumulation of ubiquitinated proteins in UBPy-deficient cells that colocalize with the enlarged endosomes might not only represent ubiquitinated conjugated substrates associated with the endosome, but could also reflect enhanced amounts of ubiquitinated cargo derived from the cell membrane. Such a functional role of UBPy exerted on cell membrane components is compatible with the cellular localization of endogenous UBPy.

As described here, the absence of UBPy caused a severe reduction of HRS. HRS binds directly to ubiquitinated proteins, which are then sorted to clathrin-coated microdomains while nonubiquitinated receptors, like transferrin or LDL receptor, are rapidly recycled to the cell surface (45). Endosomal enlargement in UBPy-deficient cells most likely can be attributed to the lack of HRS, as HRS-deficient murine cells and drosophila HRS$^{-/-}$ mutant larvae (27, 34) were also reported to exhibit this phenotype. While this work was in progress, two reports also described endosomal enlargement when UBPy was knocked down by RNA interference (7, 48), supporting an essential role of UBPy in endocytic trafficking.

As HRS itself was identified as a protein that is tyrosine phosphorylated upon stimulation with hepatocyte growth factor, platelet-derived growth factor, and epidermal growth factor (26) and HRS$^{-/-}$ drosophila pupae have reduced levels of EGFR (34), it is appealing to see a functional relationship between the lack of RTKs and the lack of HRS in UBPy-deficient cells and animals. However, the knockdown of HRS in cultured cells, as well as the combined inactivation of STAM1 and STAM2, was reported to even inhibit the degra-

dation of ligand-activated RTK degradation (4, 22, 35). Thus, the observed reduction of RTKs in UBPy$^{-/-}$ cells is unlikely to be caused by the lack of HRS but rather reflects a function of UBPy independent of the stabilization of the HRS-STAM complex. This is supported by results from Mizuno et al., who described a direct interaction of UBPy and the EGFR resulting in EGFR deubiquitination (38). The observed accumulation of MVBs shows that in UBPy$^{-/-}$ cells, endosomes can efficiently mature to MVBs even in the absence of the HRS-STAM complex, a prerequisite of RTK degradation via the lysosomal pathway.

The results suggest that UBPy exerts two independent functions in the RTK degradation pathway, first by directly counteracting RTK internalization and second by stabilizing the HRS-STAM complex. Both activities might act in concert to regulate thresholds for RTK degradation.

ACKNOWLEDGMENTS

We are particularly grateful to Ivan Dikic for suggestions and for critically reading the manuscript. We thank Marcus Wietstruk, Elvira Rhode, Melanie Benedict, Claudia Pallasch, Bianca Verrett, and Ulrike Kuckelkorn for technical assistance and Harald Stenmark, Simono Polo, Daniel Metzger, and Ivan Dikic for providing essential reagents and antibodies.

We declare that we do not have competing financial interests.

This work was supported by grant KN590/2-1 to K.-P. Knobeloch from the Deutsche Forschungsgemeinschaft.

REFERENCES

1. **Amerik, A. Y., and M. Hochstrasser.** 2004. Mechanism and function of deubiquitinating enzymes. Biochim. Biophys. Acta **1695:**189–207.
2. **Amerik, A. Y., S. J. Li, and M. Hochstrasser.** 2000. Analysis of the deubiquitinating enzymes of the yeast *Saccharomyces cerevisiae*. Biol. Chem. **381:** 981–992.
3. **Amerik, A. Y., J. Nowak, S. Swaminathan, and M. Hochstrasser.** 2000. The Doa4 deubiquitinating enzyme is functionally linked to the vacuolar protein-sorting and endocytic pathways. Mol. Biol. Cell. **11:**3365–3380.
4. **Bache, K. G., C. Raiborg, A. Mehlum, and H. Stenmark.** 2003. STAM and Hrs are subunits of a multivalent ubiquitin-binding complex on early endosomes. J. Biol. Chem. **278:**12513–12521.
5. **Bishop, N., A. Horman, and P. Woodman.** 2002. Mammalian class E vps proteins recognize ubiquitin and act in the removal of endosomal protein-ubiquitin conjugates. J. Cell Biol. **157:**91–101.
6. **Borowiak, M., A. N. Garratt, T. Wustefeld, M. Strehle, C. Trautwein, and C. Birchmeier.** 2004. Met provides essential signals for liver regeneration. Proc. Natl. Acad. Sci. USA **101:**10608–10613.
7. **Bowers, K., S. C. Piper, M. A. Edeling, S. R. Gray, D. J. Owen, P. J. Lehner, and J. P. Luzio.** 2006. Degradation of endocytosed epidermal growth factor and virally ubiquitinated major histocompatibility complex class I is independent of mammalian ESCRTII. J. Biol. Chem. **281:**5094–5105.
8. **Brummelkamp, T. R., S. M. B. Nijman, A. M. G. Dirac, and R. Bernards.** 2003. Loss of the cylindromatosis tumour suppressor inhibits apoptosis by activating NF-kappa B. Nature **424:**797–801.
9. **Feil, R., J. Brocard, B. Mascrez, M. LeMeur, D. Metzger, and P. Chambon.** 1997. Ligand-inducible gene targeting in mice. Naunyn-Schmiedebergs Arch. Pharmacol. **355:**41.
10. **Feil, R., J. Wagner, D. Metzger, and P. Chambon.** 1997. Regulation of Cre recombinase activity by mutated estrogen receptor ligand-binding domains. Biochem. Biophys. Res. Commun. **237:**752–757.
11. **Gnesutta, N., M. Ceriani, M. Innocenti, I. Mauri, R. Zippel, E. Sturani, B. Borgonovo, G. Berruti, and E. Martegani.** 2001. Cloning and characterization of mouse UBPy, a deubiquitinating enzyme that interacts with the Ras guanine nucleotide exchange factor CDC25(Mm)/Ras-GRF1. J. Biol. Chem. **276:**39448–39454.
12. **Graner, E., D. Tang, S. Rossi, A. Baron, T. Migita, L. J. Weinstein, M. Lechpammer, D. Huesken, J. Zimmermann, S. Signoretti, and M. Loda.** 2004. The isopeptidase USP2a regulates the stability of fatty acid synthase in prostate cancer. Cancer Cell **5:**253–261.
13. **Haglund, K., P. P. Di Fiore, and I. Dikic.** 2003. Distinct monoubiquitin signals in receptor endocytosis. Trends Biochem. Sci. **28:**598–603.
14. **Haglund, K., and I. Dikic.** 2005. Ubiquitylation and cell signaling. EMBO J. **24:**3353–3359.
15. **Haglund, K., S. Sigismund, S. Polo, I. Szymkiewicz, P. P. Di Fiore, and I. Dikic.** 2003. Multiple monoubiquitination of RTKs is sufficient for their endocytosis and degradation. Nat. Cell Biol. **5:**461–466.
16. **Harkiolaki, M., M. Lewitzky, R. J. C. Gilbert, E. Y. Jones, R. P. Bourette, G. Mouchiroud, H. Sondermann, I. Moarefi, and S. M. Feller.** 2003. Structural basis for SH3 domain-mediated high-affinity binding between Mona/Gads and SLP-76. EMBO J. **22:**2571–2582.
17. **Hicke, L., and R. Dunn.** 2003. Regulation of membrane protein transport by ubiquitin and ubiquitin-binding proteins. Annu. Rev. Cell Dev. Biol. **19:**141–172.
18. **Holzenberger, M., C. Lenzner, P. Leneuve, R. Zaoui, G. Hamard, S. Vaulont, and Y. L. Bouc.** 2000. Cre-mediated germline mosaicism: a method allowing rapid generation of several alleles of a target gene. Nucleic Acids Res. **28:**e92.
19. **Huang, T. T., S. M. Nijman, K. D. Mirchandani, P. J. Galardy, M. A. Cohn, W. Haas, S. P. Gygi, H. L. Ploegh, R. Bernards, and A. D. D'Andrea.** 2006. Regulation of monoubiquitinated PCNA by DUB autocleavage. Nat. Cell Biol. **8:**3309–3347.
20. **Huh, C. G., V. M. Factor, A. Sanchez, K. Uchida, E. A. Conner, and S. S. Thorgeirsson.** 2004. Hepatocyte growth factor/c-met signaling pathway is required for efficient liver regeneration and repair. Proc. Natl. Acad. Sci. USA **101:**4477–4482.
21. **Janssen, J. W. G., L. Schleithoff, C. R. Bartram, and A. S. Schulz.** 1998. An oncogenic fusion product of the phosphatidylinositol 3-kinase p85 beta subunit and HUMORF8, a putative deubiquitinating enzyme. Oncogene **16:** 1767–1772.
22. **Kanazawa, C., E. Morita, M. Yamada, N. Ishii, S. Miura, H. Asao, T. Yoshimori, and K. Sugamura.** 2003. Effects of deficiencies of STAMs and Hrs, mammalian class E Vps proteins, on receptor downregulation. Biochem. Biophys. Res. Commun. **309:**848–856.
23. **Kaneko, T., T. Kumasaka, T. Ganbe, T. Sato, K. Miyazawa, N. Kitamura, and N. Tanaka.** 2003. Structural insight into modest binding of a non-PXXP ligand to the signal transducing adaptor molecule-2 Src homology 3 domain. J. Biol. Chem. **278:**48162–48168.
24. **Kato, M., K. Miyazawa, and N. Kitamura.** 2000. A deubiquitinating enzyme UBPY interacts with the Src homology 3 domain of Hrs-binding protein via a novel binding motif PX(V/I)(D/N)RXXKP. J. Biol. Chem. **275:**37481–37487.
25. **Knobeloch, K. P., O. Utermohlen, A. Kisser, M. Prinz, and I. Horak.** 2005. Reexamination of the role of ubiquitin-like modifier ISG15 in the phenotype of UBP43-deficient mice. Mol. Cell. Biol. **25:**11030–11034.
26. **Komada, M., and N. Kitamura.** 1995. Growth factor-induced tyrosine phosphorylation of Hrs, a novel 115-kilodalton protein with a structurally conserved putative zinc finger domain. Mol.d Cell. Biol. **15:**6213–6221.
27. **Komada, M., and P. Soriano.** 1999. Hrs, a FYVE finger protein localized to early endosomes, is implicated in vesicular traffic and required for ventral folding morphogenesis. Genes Dev. **13:**1475–1485.
28. **Kovalenko, A., C. Chable-Bessia, G. Cantarella, A. Israel, D. Wallach, and G. Courtois.** 2003. The tumour suppressor CYLD negatively regulates NF-kappa B signalling by deubiquitination. Nature **424:**801–805.
29. **Kuhn, R., F. Schwenk, M. Aguet, and K. Rajewsky.** 1995. Inducible gene targeting in mice. Science **269:**1427–1429.
30. **Lakso, M., J. G. Pichel, J. R. Gorman, B. Sauer, Y. Okamoto, E. Lee, F. W. Alt, and H. Westphal.** 1996. Efficient in vivo manipulation of mouse genomic sequences at the zygote stage. Proc. Natl. Acad. Sci. USA **93:**5860–5865.
31. **Li, L. M., and S. N. Cohen.** 1996. tsg101: a novel tumor susceptibility gene isolated by controlled homozygous functional knockout of allelic loci in mammalian cells. Cell **85:**319–329.
32. **Li, M. Y., C. L. Brooks, N. Kon, and W. Gu.** 2004. A dynamic role of HAUSP in the p53-Mdm2 pathway. Mol. Cell **13:**879–886.
33. **Li, M. Y., D. L. Chen, A. Shiloh, J. Y. Luo, A. Y. Nikolaev, J. Qin, and W. Gu.** 2002. Deubiquitination of p53 by HAUSP is an important pathway for p53 stabilization. Nature **416:**648–653.
34. **Lloyd, T. E., R. Atkinson, M. N. Wu, Y. Zhou, G. Pennetta, and H. J. Bellen.** 2002. Hrs regulates endosome membrane invagination and tyrosine kinase receptor signaling in *Drosophila*. Cell **108:**261–269.
35. **Lu, Q., L. W. Q. Hope, M. Brasch, C. Reinhard, and S. N. Cohen.** 2003. TSG101 interaction with HRS mediates endosomal trafficking and receptor down-regulation. Proc. Natl. Acad. Sci. USA **100:**7626–7631.
36. **Matsuo, H., J. Chevallier, N. Mayran, I. Le Blanc, C. Ferguson, J. Faure, N. S. Blanc, S. Matile, J. Dubochet, M. Sadoul, R. G. Parton, F. Vilbois, and J. Gruenberg.** 2004. Role of LBPA and Alix in multivesicular liposome formation and endosome organization. Science **303:**531–534.
37. **Millard, S. M., and S. A. Wood.** 2006. Riding the DUBway: regulation of protein trafficking by deubiquitylating enzymes. J. Cell Biol. **173:**463–468.
38. **Mizuno, E., T. Iura, A. Mukai, T. Yoshimori, N. Kitamura, and M. Komada.** 2005. Regulation of epidermal growth factor receptor down-regulation by UBPY-mediated deubiquitination at endosomes. Mol. Biol. Cell **16:**5163–5174.
39. **Mosesson, Y., K. Shtiegman, M. Katz, Y. Zwang, G. Vereb, J. Szollosi, and Y. Yarden.** 2003. Endocytosis of receptor tyrosine kinases is driven by monoubiquitylation, not polyubiquitylation. J. Biol. Chem. **278:**21323–21326.
40. **Naviglio, S., C. Matteucci, B. Matoskova, T. Nagase, N. Nomura, P. P. Di**

Fiore, and G. F. Draetta. 1998. UBPY: a growth-regulated human ubiquitin isopeptidase. EMBO J. **17:**3241–3250.
41. **Nijman, S. M. B., T. T. Huang, A. M. G. Dirac, T. R. Brummelkamp, R. M. Kerkhoven, A. D. D'Andrea, and R. Bernards.** 2005. The deubiquitinating enzyme USP1 regulates the Fanconi anemia pathway. Mol. Cell **17:**331–339.
42. **Nijman, S. M. B., M. P. A. Luna-Vargas, A. Velds, T. R. Brummelkamp, A. M. G. Dirac, T. K. Sixma, and R. Bernards.** 2005. A genomic and functional inventory of deubiquitinating enzymes. Cell **123:**773–786.
43. **Osiak, A., O. Utermohlen, S. Niendorf, I. Horak, and K. P. Knobeloch.** 2005. ISG15, an interferon-stimulated ubiquitin-like protein, is not essential for STAT1 signaling and responses against vesicular stomatitis and lymphocytic choriomeningitis virus. Mol. Cell. Biol. **25:**6338–6345.
44. **Pickart, C. M.** 2001. Mechanisms underlying ubiquitination. Annu. Rev. Biochem. **70:**503–533.
45. **Raiborg, C., K. G. Bache, D. J. Gillooly, I. H. Madshush, E. Stang, and H. Stenmark.** 2002. Hrs sorts ubiquitinated proteins into clathrin-coated microdomains of early endosomes. Nat. Cell Biol. **4:**394–398.
46. **Raiborg, C., K. G. Bache, A. Mehlum, E. Stang, and H. Stenmark.** 2001. Hrs recruits clathrin to early endosomes. EMBO J. **20:**5008–5021.
47. **Reiley, W. W., M. Y. Zhang, W. Jin, M. Losiewicz, K. B. Donohue, C. C. Norbury, and S. C. Sun.** 2006. Regulation of T cell development by the deubiquitinating enzyme CYLD. Nat. Immunol. **7:**411–417.
48. **Row, P. E., I. A. Prior, J. McCullough, M. J. Clague, and S. Urbe.** 2006. The ubiquitin isopeptidase UBPY regulates endosomal ubiquitin dynamics and is essential for receptor down-regulation. J. Biol. Chem. **281:**12618–12624.
49. **Schumann, G., R. Bonora, F. Ceriotti, G. Ferard, C. A. Ferrero, P. F. H. Franck, F. J. Gella, W. Hoelzel, P. J. Jorgensen, T. Kanno, A. Kessner, R. Klauke, N. Kristiansen, J. M. Lessinger, T. P. J. Linsinger, H. Misaki, M. Panteghini, J. Pauwels, F. Schiele, H. G. Schimmel, G. Weidemann, and L. Siekmann.** 2002. IFCC primary reference procedures for the measurement of catalytic activity concentrations of enzymes at 37°C. Part 5. Reference procedure for the measurement of catalytic concentration of aspartate aminotransferase. Clin. Chem. Lab. Med. **40:**725–733.
50. **Soares, L., C. Seroogy, H. Skrenta, N. Anandasabapathy, P. Lovelace, C. D. Chung, E. Engleman, and C. G. Fathman.** 2004. Two isoforms of otubain 1 regulate T cell anergy via GRAIL. Nat. Immunol. **5:**45–54.
51. **Takata, H., M. Kato, K. Denda, and N. Kitamura.** 2000. A Hrs binding protein having a Src homology 3 domain is involved in intracellular degradation of growth factors and their receptors. Genes Cells **5:**57–69.
52. **Trompouki, E., E. Hatzivassiliou, T. Tsichritzis, H. Farmer, A. Ashworth, and G. Mosialos.** 2003. CYLD is a deubiquitinating enzyme that negatively regulates NF-kappa B activation by TNFR family members. Nature **424:**793–796.
53. **Welchman, R. L., C. Gordon, and R. J. Mayer.** 2005. Ubiquitin and ubiquitin-like proteins as multifunctional signals. Nat. Rev. Mol. Cell Biol. **6:**599–609.
54. **Williams, D. A., W. Tao, F. C. Yang, C. Kim, Y. Gu, P. Mansfield, J. E. Levine, B. Petryniak, C. W. Derrow, C. Harris, B. Q. Jia, Y. Zheng, D. R. Ambruso, J. B. Lowe, S. J. Atkinson, M. C. Dinauer, and L. Boxer.** 2000. Dominant negative mutation of the hematopoietic-specific Rho GTPase, Rac2, is associated with a human phagocyte immunodeficiency. Blood **96:**1646–1654.
55. **Wu, X. L., L. Yen, L. Irwin, C. Sweeney, and K. L. Carraway.** 2004. Stabilization of the E3 ubiquitin ligase Nrdp1 by the deubiquitinating enzyme USP8. Mol. Cell. Biol. **24:**7748–7757.